

of magnitude of the starred terms to insure stability. Noting this, and eliminating  $\omega_2^*$  from the two remaining equations of motion leads to the equation

$$(I_2 + I)(I_3 + I)(d^2\omega_3^*/dt^2) + \{\omega_0^2[(I_1 - I_3)(I_1 - I_2) + I(2I_1 - I_2 - I_3) + I^2] + 2\omega_0 I(2I + 2I_1 - I_2 - I_3)Ap \cos pt\} \omega_3^* = 0 \quad (18)$$

which may be written easily in the form

$$(d^2\omega_3^*/dt^2) + (\delta + \epsilon \cos t) \omega_3^* = 0 \quad (19)$$

Furthermore, it easily is shown that by eliminating  $\omega_3^*$  from the motion equations leads to an identical equation for  $\omega_2^*$ .

The conditions for stability of this Mathieu equation are well known and may be found, for example, in Stoker's "Non-linear Vibrations".<sup>3</sup> Basically, the stability depends upon the values of  $\delta$  and  $\epsilon$ . It is known that by proper choice of  $\epsilon$ , stability may be attained even for negative  $\delta$  and also instability may be attained for positive  $\delta$ .

### Discussion

In the first case considered, it is seen in Eq. (15) that, if no gyro were present, that is, if  $I$  is vanishingly small, there would be stability of rotation only if the axis of rotation is parallel to a maximum or minimum inertia axis of the vehicle for its mass center. This is a well-known result. However, with a rotating gyro within the vehicle, it is clear that stability may be attained irrespective of the inertia properties or rotation of the vehicle by simply making the product  $I\Omega$  large enough.

In the second case, it is seen in Eq. (18) or (19) that rotational stability of the vehicle may be attained (or disrupted) simply by oscillation of the gyro, the stability being dependent upon the frequency and amplitude of oscillation.

### References

- <sup>1</sup> Kane, T. R., *Analytical Elements of Mechanics* (Academic Press Inc., New York, 1961), Vol. 2, pp. 177-178.
- <sup>2</sup> Kane, T. R., *Analytical Element of Mechanics* (Academic Press Inc., New York, 1961), Vol. 2, p. 61.
- <sup>3</sup> Stoker, J. J., *Nonlinear Vibrations* (Interscience Publishers Inc., New York, 1950), pp. 202-213.

## Approximations for Supersonic Flow over Cones

WAYNE E. SIMON\* AND LOUISE A. WALTER†  
Martin Company, Denver, Colo.

### Nomenclature

- $C_p$  = surface pressure coefficient  
 $f_1, f_2, f_3$  = functions defined by Eqs. (3-5)  
 $g_1, g_2, g_3$  = functions defined by Eqs. (6-8)  
 $M$  = Mach number  
 $\gamma$  = ratio of specific heats  
 $\delta$  = cone angle  
 $\theta$  = shock wave angle

### Subscripts

- $\infty$  = freestream conditions  
 $c$  = conditions on cone surface  
 $M$  = conditions at the largest cone angle that permits an attached shock

Received April 15, 1963.

\* Associate Research Scientist, Aerospace Division of Martin Marietta Corporation. Member AIAA.

† Senior Engineer, Aerospace Division of Martin Marietta Corporation.

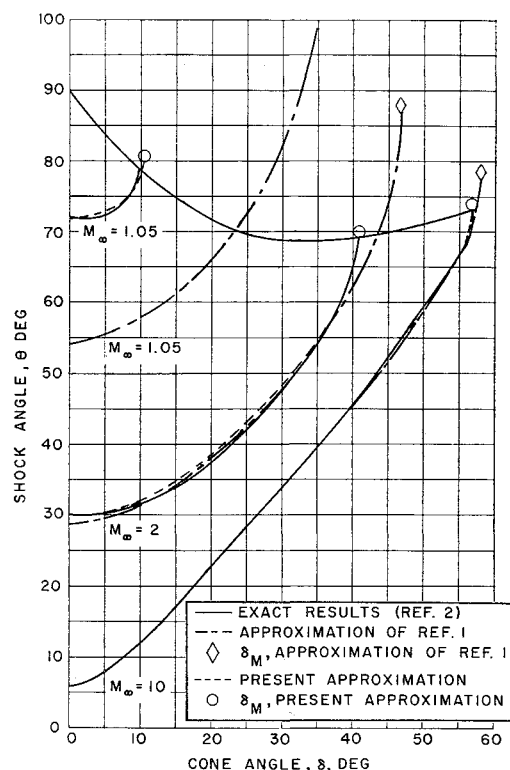


Fig. 1 Comparison of shock angle approximations ( $\gamma = 1.405$ )

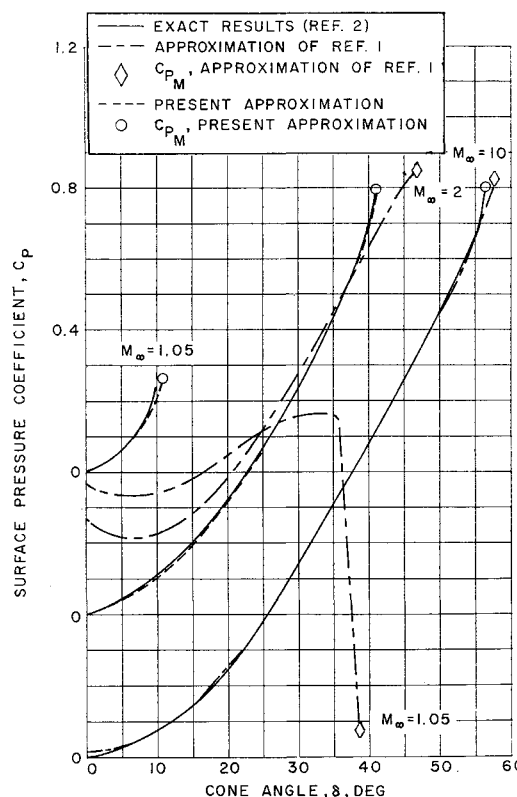


Fig. 2 Comparison of surface pressure coefficient approximations ( $\gamma = 1.405$ )

IN many applications, it is necessary to compute the shock angle, surface pressure, and surface Mach number for a cone at zero angle of attack in supersonic flow. The independent variables are freestream Mach number, cone angle, and specific heat ratio of the gas. Generally, three courses of action are possible. First, the differential equation of the flow could be solved for each case. Second, tables of solu-

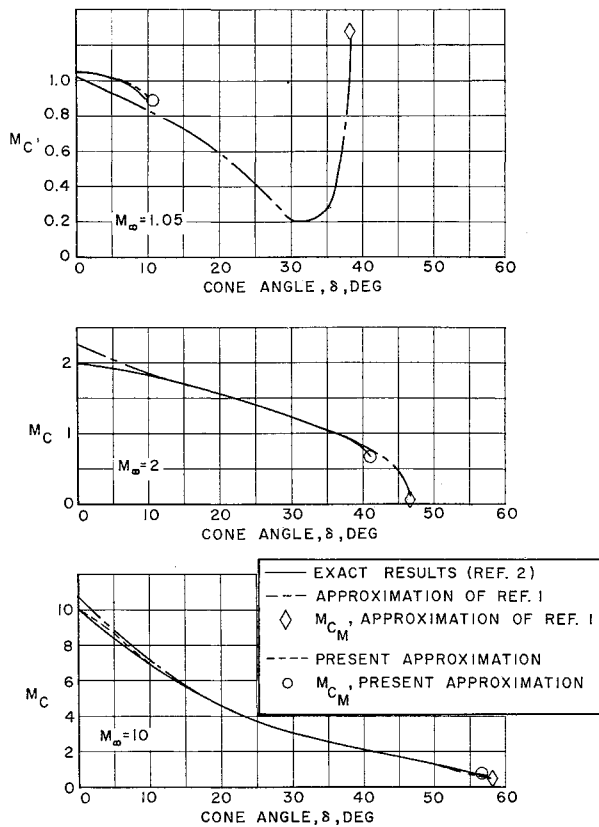


Fig. 3 Comparison of surface Mach number approximations ( $\gamma = 1.405$ )

tions could be used, with interpolation for each case. Third, some analytical approximation could be used. In a computer application, the first method takes a good deal of time, and the second takes a large amount of computer memory. Thus, if sufficient precision can be obtained, the third method is very attractive.

On the basis of  $M_\infty \gg 1$ , Ref. 1 develops approximate solutions for conical flow. However, the results are good approximations only if  $M_\infty > 10$ . It is possible to take a somewhat different approach to the problem of approximation. Instead of developing approximate solutions for certain limiting conditions, one can look at the form of the results given by Ref. 2, which are tabulated and graphed results of solutions of the differential equation. Careful examination shows that the variations in surface pressure coefficient and shock wave angle are nearly quadratic, and after some trial and error, the following approximations can be determined.

$$C_p = \frac{1}{2}(f_2 + f_1 \sin^2 \delta - \{(f_2 - f_1 \sin^2 \delta)^2 - [(f_3 - f_1) \sin^2 \delta]^2\}^{1/2}) \quad (1)$$

$$\sin^2 \theta = (1/M_\infty^2) + \frac{1}{2}(g_2 + g_1 \sin^2 \delta - \{(g_2 - g_1 \sin^2 \delta)^2 - [(g_3 - g_1) \sin^2 \delta]^2\}^{1/2}) \quad (2)$$

where

$$f_1(M_\infty, \gamma, \delta) = \left(\frac{\gamma + 7}{4}\right) - \left(\frac{\gamma - 1}{4}\right)^2 + \frac{6}{M_\infty^6} + \frac{M_\infty^2 - 1}{M_\infty^4 \sin \delta} \quad (3)$$

$$f_2(M_\infty, \gamma) = \frac{1}{2} \left(\frac{\gamma + 7}{\gamma + 1}\right) \left(1 - \frac{1}{M_\infty^2}\right) \left(1 + \frac{1}{M_\infty^6}\right) \quad (4)$$

$$f_3(M_\infty, \gamma) = \frac{\gamma}{2} \left(\frac{\gamma + 7}{\gamma + 1}\right) \left(1 + \frac{1}{M_\infty^2}\right) \left(1 + \frac{1}{M_\infty^6}\right) \quad (5)$$

$$g_1(\gamma) = (\gamma + 1)/2 \quad (6)$$

$$g_2(M_\infty) = 1 - (1/M_\infty^2) \quad (7)$$

$$g_3(M_\infty, \gamma) = \gamma[1 + (1/M_\infty^2)] \quad (8)$$

If the subscript  $M$  is used to mean the conditions for the largest cone angle which permit an attached shock, then

$$\sin^2 \delta_M = g_2/g_3 \quad (9)$$

$$\sin^2 \theta_M = (1/M_\infty^2) + \frac{1}{2}[g_2 + (g_1 g_2/g_3)] \quad (10)$$

$$C_{pM} = \frac{1}{2}[f_2 + (f_1 g_2/g_3)] \quad (11)$$

Finally, it is noted that if  $\sin \delta < 0.85 \sin \delta_M$ , Eqs. (1) and (2) may be further approximated to give

$$C_p = f_1 \sin^2 \delta \quad (12)$$

$$\sin^2 \theta = (1/M_\infty^2) + g_1 \sin^2 \delta \quad (13)$$

Note that given  $\theta$  and  $C_p$ , the usual flow relations can be used to compute surface Mach number.

Figure 1 presents a comparison of the two shock angle approximations with exact results. It is seen that for higher Mach numbers, and for cone angles well below the maximum, both approximations are good. However, the present approximation works well for all Mach numbers and for cone angles up to and including the detachment angle.

Figures 2 and 3 present the same comparison for surface pressure coefficient and surface Mach number. The same characteristics of the two approximations show up in these figures.

In Figs. 1-3, it will be noted that the approximation of Ref. 1 gives results for shock angle, pressure coefficient, and surface Mach number beyond the limit for an attached shock wave as predicted by theory and the present approximation. These results are shown in order to give comparisons at predicted shock detachment angle for the two approximations and exact theory.

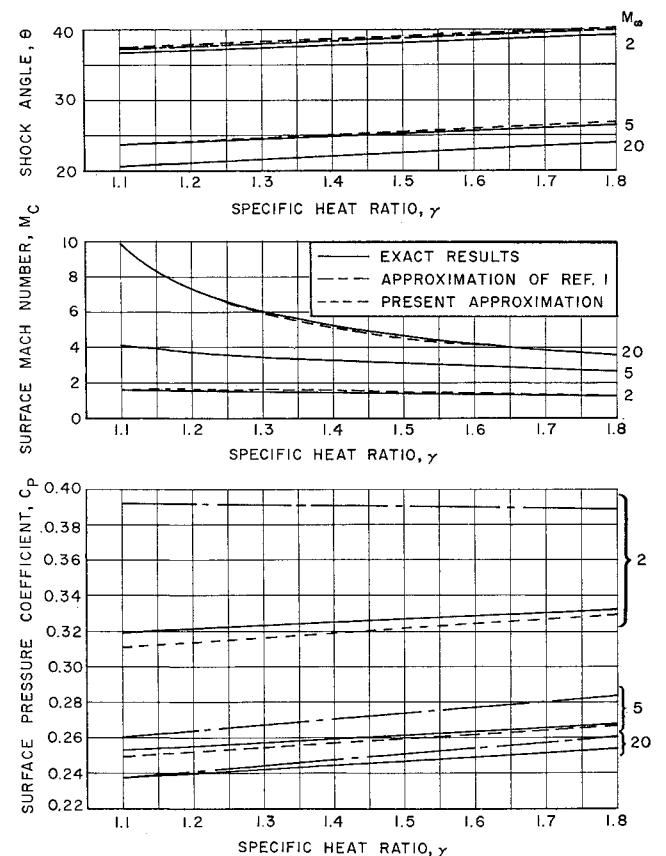


Fig. 4 Comparison of shock angle, surface pressure coefficient, and surface Mach number approximations at various  $\gamma$  ( $\delta = 20^\circ$ )

Figure 4 presents comparison of the effects of specific heat ratio for a cone angle of  $20^\circ$ . Both approximations are close for shock angle and surface Mach number, but the approximation of Ref. 1 shows appreciable error in surface pressure coefficient, even for  $M_\infty = 20$ .

Approximations for shock wave angle and surface pressure coefficient, which can be used for all Mach numbers and for cone angles from zero to the detachment value, have been determined for the case of a cone at zero angle of attack in supersonic flow. Comparisons with exact results indicate that the precision is adequate for engineering purposes.

### References

<sup>1</sup> Hammitt, A. G. and Murthy, K. R. A., "Approximate solutions for supersonic flow over wedges and cones," J. Aerospace Sci. 27, 71-72 (1960).

<sup>2</sup> "Equations, tables, and charts for compressible flow," Ames Res. Lab., NACA Rept. 1135, pp. 48-53 (1953).

## Travel Summation and Time Summation Methods of Free-Oscillation Data Analysis

KAZIMIERZ J. ORLIK-RÜCKEMANN\*  
National Aeronautical Establishment,  
Ottawa, Ontario, Canada

THERE are many instances, e.g., when performing wind tunnel studies of the dynamic behavior of re-entry configurations, where experiments involving very large amplitudes of oscillation are of interest. In such cases, it may be difficult to obtain data in the convenient form of an analog output of the displacement-time history, and hence the instantaneous methods of data reduction such as the dampometer method<sup>1</sup> or the integration method<sup>2</sup> cannot be used. The two methods described herein do not require analog outputs yet still permit instantaneous reduction of free-oscillation data. They are both based on the concept of viscous damping and thus present results in terms of the equivalent viscous damping.

### Travel Summation Method

It will be shown here, that if the sum of all the travel segments between two preset levels of displacement of a free decaying oscillation is known, the logarithmic decrement corresponding to the equivalent viscous damping can be obtained from a simple analytical expression.

In order to visualize more easily the problem, one can consider the simplest form of many possible experimental arrangements, namely an oscillating light source seen through a stationary window, as schematically presented in Fig. 1. The length of the window and its position are such that the light source can be seen only during a portion of each cycle, namely when its deflection from equilibrium is between  $x_0$  and  $x_m$ . When the amplitude of oscillation decreases below  $x_m$  the light source is cut off. The total visible travel of the light source in relation to the window is recorded. This can be done, e.g., by replacing the window with a large number of fine transversal slots and recording the total number of resulting light pulses on a photomultiplier tube. The procedure, of course, can be applied to both translational and angular oscillatory motions; it can be reversed by keeping

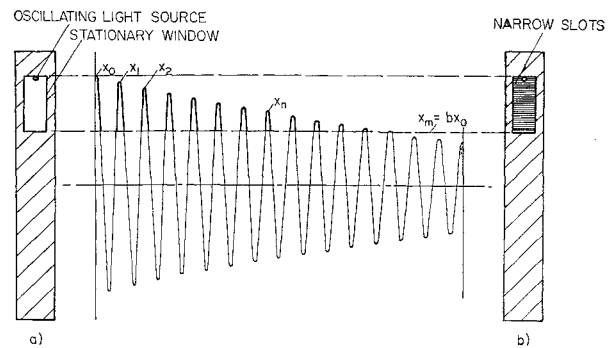


Fig. 1 Free oscillation data analysis using a) time summation method [Eqs. (9, 10, and 13)] and b) travel summation method [Eqs. (3, 4, and 7)]

the light source stationary and oscillating the slotted window; it can be modified by keeping both the light source and the slotted window stationary and oscillating suitably located mirrors. Numerous experimental arrangements are possible, but their detail aspects will not be elaborated here.

Thus, if the upper limit of the amplitude range under consideration is  $x_0$  and the lower limit is  $x_m$ , one has, for a free-oscillation motion with viscous damping,

$$x_m = e^{-m\delta}x_0 = c^m x_0 = b x_0 \quad (1)$$

where  $m$  denotes the number of cycles between  $x_0$  and  $x_m$  and  $c = e^{-\delta}$  is a convenient constant related to the amount of viscous damping;  $\delta$  denotes the logarithmic decrement. The amplitude of the  $n$ th peak between  $x_0$  and  $x_m$  similarly can be written as

$$x_n = c^n x_0 \quad (2)$$

Assuming that the oscillation starts at  $x_0$ , the sum  $S$  of all the travel segments contained between  $x_0$  and  $x_m$  is

$$S = 2 \sum_{n=0}^m (x_n - x_m) - (x_0 - x_m) \quad (3)$$

Inserting Eqs. (1) and (2) and expressing the total travel  $S$  in terms of the initial amplitude  $x_0$ , one obtains

$$s = \frac{S}{x_0} = 2 \sum_{n=0}^m c^n - (2m+1)b - 1 \quad (4)$$

Replacing the geometric progression on the right-hand side by its sum and solving for  $c$ , one gets

$$c = \frac{s + (2m+1)b - 1}{s + (2m+1)b - 2b + 1} = \frac{1 - [(1-b)/(s+2mb)]}{1 + [(1-b)/(s+2mb)]} \quad (5)$$

The logarithmic decrement now can be obtained from

$$\delta = \ln \frac{1}{c} = 2 \left[ \left( \frac{1-b}{s+2mb} \right) + \frac{1}{3} \left( \frac{1-b}{s+2mb} \right)^3 + \dots \right] \quad (6)$$

where for most applications only the first term of the logarithmic expansion need be retained. The resulting error is less than 0.1% for  $\delta < 0.1$  and less than 0.8% for  $\delta < 0.3$ .

Using the relation between  $m$ ,  $b$ , and  $\delta$  given by Eq. (1),  $m$  can be eliminated, which leads to the final expression for the logarithmic decrement

$$\delta = (2/s)(1 - b + b \ln b) \quad (7)$$

For a given experimental arrangement  $b$  is fixed (with convenient values around 0.5), and thus the logarithmic decrement is simply obtained by dividing a constant by the dimensionless sum  $s$  of the travel segments. It should be noted that, since a change in  $b$  causes a change in the travel segment

Received April 22, 1963.

\* Head, Unsteady Aerodynamics Laboratory. Associate Fellow Member AIAA.